Asia-Pacific Journal of Science and Technology: Volume: 28. Issue: 03. Article ID.: APST-28-03-02. Research Article

APST

Asia-Pacific Journal of Science and Technology

https://www.tci-thaijo.org/index.php/APST/index

Published by the Research and Graduate Studies,
Khon Kaen University, Thailand

A study of co-doping of rare earth and alkaline earth metals with zinc oxide nanoparticles

Parvathy Bhaskar[1,*], Mg Veena[1] and Bs Madhukar[1]

[1]Department of Electronics and Communication Engineering, Sri Jayachamarajendra College of Engineering, JSS Science and Technology University, Karnataka, India
[*]Corresponding author: parvathybhaskar@jssstuniv.in

Received 9 March 2022
Revised 27 April 2022
Accepted 28 April 2022

Abstract

The current paper sums up the findings of the synthesis and the resultant properties of thorium (Th) doped zinc oxide (ZnO) nano powder with co-doping of magnesium (Mg) and calcium (Ca), by the solution combustion synthesis method. The structural, morphological, and elemental analyses of the synthesized nanoparticles were examined by powder x-ray diffraction (PXRD), high-resolution transmission electron microscopy (HRTEM) with selected area electron diffraction (SAED) patterns and field emission scanning electron microscopy with energy dispersive x-ray spectroscopy (FESEM/EDX). The optical properties were studied using ultraviolet visible near infra-red (UV-vis NIR) spectroscopy. The doped samples exhibited enhanced photocatalytic activity. The PXRD spectra confirmed the crystalline nature of the samples, and the pure ZnO samples exhibited an average grain size of 42 nm. While the Th doped samples had a grain size of 20.03 nm, those of the samples co-doped with Mg and Ca grain size were 24.63 nm and 28.6 nm respectively. Thus, with doping, the grain size decreased while the crystallinity remained the same. The elemental composition analysis revealed that the elements on the surface of the prepared samples were zinc. The surface topography and morphology were studied by atomic force microscopy (AFM) which showed the homogenous distribution of the particles.

Keywords: Band gap, Co-doping, Energy dispersive spectroscopy, Rare earth, Solution combustion synthesis

1. Introduction

With the fast growth of nanoscience and technology, many mellitic oxides have attracted the attention of researchers, and among them Zinc oxide (ZnO) is the most prominent one. ZnO is cheap and exhibits semiconductor properties with band gap of 3.37 electron volt (eV), fabrication flexibility and tunable properties. Hence it has wide applications in nano scale engineering. Metal oxide semiconductors doped with rare earths are found to have excellent size and shape-dependent properties, which open up huge possibilities of utility in the fields of power storage, optoelectronics, photovoltaic cells, photocatalysts, biomedical applications, semiconductor electronics, power electronics and varistor application devices. In ZnO nanoparticles, the structural, optical, and electrical properties are greatly affected by the presence of impurities like the rare earth and alkaline earth metals, but these properties can be tuned by varying the impurity concentration. Of late, ZnO nanoparticles have acquired technological importance in the area of spintronics due to their ferromagnetic properties when doped with transition metals [1]. The structural and morphological properties generally depend on the process of synthesis. Furthermore, the doping element and its composition alter the electrical conductivity and the band gap energy [2]. Moreover, by varying the dopants we can tailor the band gap to meet our application requirements.

There are various techniques for the synthesis of metal oxide nanoparticles, such as sol-gel, spray pyrolysis, co-precipitation and microwave-assisted methods. These methods cause environmental risks, involve hazardous and toxic chemicals, and are characterized by high energy consumption. Hence in this work we attempted to synthesize nanoparticles by using the solution combustion synthesis (SCS) process, which involves low

temperature and low cost [3]. Being environment-friendly, this can be considered as green synthesis since the byproducts are nontoxic gases. The SCS was discovered in the 1980s and ever since has been found suitable for synthesis of metal oxides, alloys, and sulphate nanoparticles. This process is called self-propagating combustion mode. The precursor gel is locally heated to around 500-800℃ to initiate the exothermic reaction, which propagates to form a combustion wave. To summarize, the sequence involved heating, evaporation of the precursor to form the gel, self-ignition, and combustion to form the nanoparticles. Before long, SCS methods and products will find enormous applications in mass industrial production, by customizing the combustion process and reaction conditions. Solution combustion synthesis process is the most widely used method for the preparation of a wide array of metal oxide nanoparticles. Its benefits are that it is fast, uses relatively simple equipment, forms high-purity products of any shape and size, and allows stabilization of metastable phases. Moreover, it is very effective in remediation of environmental toxins. The conventional processes require long processing time and hence consume more time and energy. There will also be a high level of polluting emissions. These processes are expensive, and large inventories will be needed to reduce costs.

There is plenty of literature as well as reports of recent work carried out by researchers on doped ZnO nanostructures. According to Rashid et al [4] copper doped ZnO nanostructures were prepared by chemical precipitation method and the researchers explored the enhanced photocatalytic and antibacterial properties of ZnO. Ali et al [5] prepared nickel and cobalt doped ZnO nanoparticles in different weight ratios and confirmed that the doped nano catalysts have better catalytic action. They used sol-gel synthesis technique and claimed that this method prevented environmental pollution issues [5]. Afzal et al [6] studied graphene oxide doped with ZnO nanoparticles using chemical deposition method and investigated their potential applications in drug delivery and drug release. Shaheen et al [7] analyzed different concentrations of graphene oxide with ZnO nanostructures by co-precipitation method and studied their photocatalytic activity. Ikram et al [8] looked into the green synthesis of ZnO nanoparticles doped with ginger and garlic roots and their applications as anti bacterials. Ikram et al [9]. prepared magnesium (Mg) doped ZnO nanorods by co-precipitation synthesis method to improve the photocatalytic properties of undoped ZnO nanostructures.

Here we discuss the effect of co-doping of thorium (Th) and alkali metal oxide calcium oxide (CaO) and magnesium oxide (MgO) on the morphological, structural, and optical properties of ZnO nanoparticles. ZnO nanoparticles with Th doping are studied since much exploration has not been done by researchers in this area. Moreover, a thorough literature survey shows that there is very little literature on Th oxide and doped Th oxide nanoparticles. This research proves that it is possible to synthesize a multifunctional nano particle in a single material by using ecofriendly, low-cost, and low-temperature solution combustion synthesis method, while still retaining the hexagonal structure of ZnO nanoparticle.

2. Materials and methods

2.1 Preparation of nanoparticles

All chemicals used were of analytical grade 99.9% purity. Metal nitrates were selected as oxidizers and glycine was used as fuel, with distilled water as the solvent in alkaline medium, without further purification. By maintaining the oxidizer-to-fuel ratio as one, the required stoichiometric ratios of zinc nitrate hexahydrate ($Zn(NO_3)_2.6H_2O$), thorium nitrate ($Th(NO_3)_4$), magnesium nitrate ($Mg(NO_3)_2$), and calcium nitrate ($Ca(NO_3)_2$), along with glycine ($C_2H_5NO_2$) were dissolved in required amounts of distilled water with alkaline pH. The precursor was magnetically stirred on a hot plate at 50℃ for 2 h until the precursor was transformed into gel form. This gel was then put into an electric crucible and heated to 500℃ to start the self-combustion process until a homogeneous metal oxide powder was obtained [3,10]. The schematic diagram of the synthesis of nanoparticles by solution combustion synthesis process is given in Figure 1. The balanced chemical reaction of the synthesis of zinc thorium oxide ($ZnThO_3$) nanoparticle by solution combustion synthesis method is as shown in Equation 1.

$$Zn(NO_3)_2 + Th(NO_3)_4 + 4C_2H_5O_2N + 3/2O_2 \longrightarrow ZnThO_3 + 8CO_2 + 10H_2O + 5N_2 \quad (1)$$

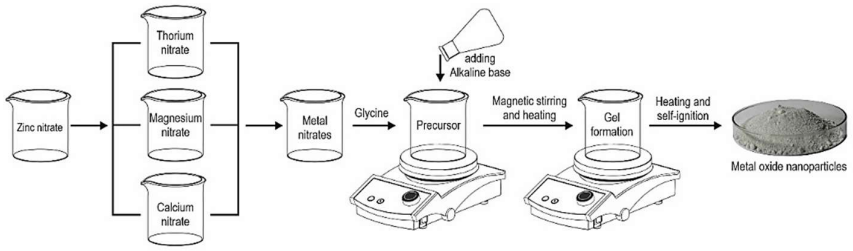

Figure 1 The preparation of nanoparticles.

2.2 Characterization techniques

The crystallinity of the synthesized samples, ZnO (100 % by weight), ZnO: Th (90:10% by weight), ZnO: Th: Mg (90:6:4% by weight), ZnO: Th: Ca (90:6:4% by weight) was evaluated using powder x-ray diffraction spectroscopy (PXRD) (Bruker D8 Advance, Germany), and morphology observed using high resolution transmission electron microscope with selected area electron diffraction (HRTEM/SAED) analysis (Joel/JEM 2100, Japan). The morphology as well as the structural and elemental information was further studied by field emission scanning electron microscope with energy dispersive x-ray spectrometer (FESEM/EDX) (Tescan-Mira 3 LMH, Czech Republic/Bruker quant ax 200, Germany). The optical properties were estimated using UV- vis NIR spectroscopy using Thermo scientific Nicolet i550 instrument (United States). To further confirm the chemical composition of the Th doped ZnO sample, an x-ray photoelectron spectroscopy (XPS-Thermo scientific ESCALAB Xi, United States) was conducted in order to assess the chemical state of the sample. The information regarding the topology of the surface was investigated using an atomic force microscope (AFM) Bruker Dimension Edge, Germany for pure ZnO and Th doped ZnO samples.

3. Results and discussion

3.1 Structural studies - powder x-ray diffraction spectroscopy

Figure 2A shows the PXRD spectra of the prepared samples in the range of 2 theta 20-90 degrees. The sharp and intense peaks confirm the high degree of crystallinity of the pure and doped samples. All the doped samples retained the hexagonal structure of the major ZnO sample. The introduction of small amounts of dopants does not bring any relevant changes in the fingerprint peaks of ZnO. The bare ZnO diffraction spectrum displayed a maximum intensity at 36.305^0 in the crystallographic (101) orientation, in accordance with Joint Committee on Powder Diffraction Standards (JCPDS) card number 01-089-0510 [1]. The peaks shifted to the lower angle side due to the presence of the dopants and got slightly broadened. The average grain size was calculated using the Debye-Scherrer equation.

$$D = k \lambda / \beta \cos \theta \quad (2)$$

where D - average crystallite size, K - Crystalline shape factor (0.9), λ - 1.54060 for Cukα (copper k-alpha electrode), θ - Angle at maximum peak, β - full width at half maximum (FWHM) of diffraction angle in radians [10]. Pure ZnO showed an average grain size of 42 nm. The nanoparticles doped with Th exhibited a very small grain size, with an average of 20.03 nm. When the samples were co-doped with Mg and Ca, the average grain sizes were found to increase to 24.63 and 28.62 respectively, accounting for the ionic radius of the dopants. Besides, it was noted that the intensity of the diffraction peaks got reduced when pure ZnO was doped with Th and co-doped with Th - Mg and Th - Ca [10-12].

The structure and the structural parameters were evaluated using Rietveld refinement (Full Prof software) and the packing diagram drawn in Visualisation for electronic structural analysis (VESTA) software. Figures 2B-D show the refinement of ZnO: Th (90:10% by weight), ZnO:Th:Mg (90:6:4% by weight) and the packing diagram [2]. It is clear from the XRD data that with the addition of Th oxide into ZnO, the lattice parameters (a=b) changed from 3.2490 A^0 to 3.18114 A^0, cell parameter (c) from 5.2050 A^0 to 5.09572 A^0 [10-12]. When co-doped with Mg oxide, the lattice parameter changed to 3.18232 A^0 and cell parameter to 5.09254 A^0 and with Ca co-doping the parameters changed to 3.24780 and 5.20018 respectively [13-15]. The parameters are listed in Table 1.

Table 1 Lattice constants calculated from XRD.

Sample composition	Lattice constant a (A^0)	Lattice constant c (A^0)
100% ZnO	3.2490	5.2050
Th doped ZnO	3.1811	5.0957
Th/Mg co-doped ZnO	3.1823	5.0925
Th/Ca co-doped ZnO	3.2478	5.2001

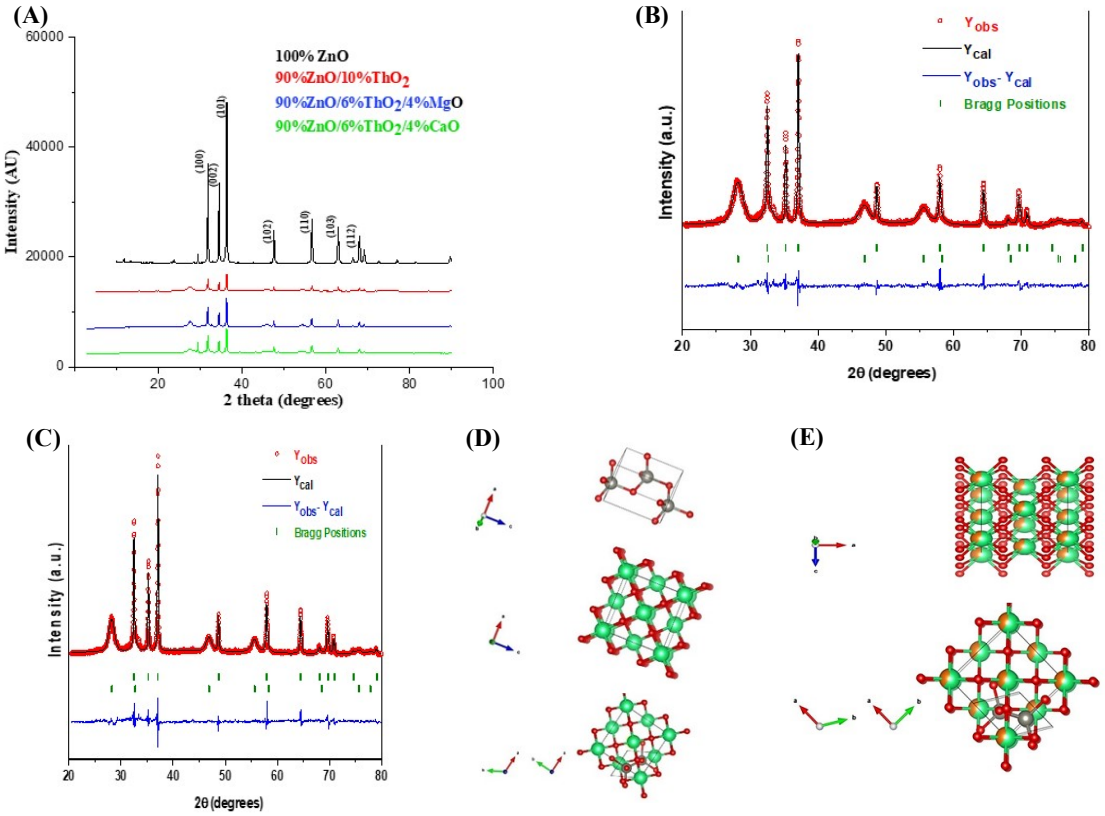

Figure 2 (A) PXRD spectra of the samples, (B) Rietveld refinement ZnO: Th, (C) Rietveld refinement ZnO: Th: Mg, (D) Packing diagram of ZnO: Th, and (E) Packing diagram of ZnO: Th: Mg.

3.2 Morphological studies HRTEM/SAED analysis

The TEM micrographs and the SAED patterns of the samples are shown in Figures 3 (A-H). The morphology of all the samples was similar to pure ZnO and showed the polycrystalline nature of the samples, thus proving that the dopant ions had not disturbed the ZnO lattice [10-12]. The average grain sizes calculated from XRD, and TEM are given in Table 2. Both the analytical techniques, XRD and TEM proved that there was very less deviation in the results with respect to crystallinity and particle size.

Table 2 Average grain size calculated from XRD and TEM.

Samples	Average crystal size from XRD (nm)	Average crystal size from TEM (nm)
100% ZnO	44.90	42
Th doped ZnO	20.03	17
Th/Mg co-doped ZnO	24.63	21
Th/Ca co-doped ZnO	28.62	25

3.3 Elemental analysis - field emission scanning electron microscopy with energy dispersive x-ray spectroscopy

The elemental and structural information was further investigated using FESEM/EDX. The EDX spectra are shown in Figures 4A-D. The spectra indicated the presence of zinc and oxygen (O_2) in ZnO sample, zinc, Th and O_2 in ZnO: Th sample, zinc, Th, Mg and O_2 in ZnO: Th: Mg sample and zinc, Th, Ca and O_2 in ZnO: Th: Ca sample. This analysis indicated the absence of any impurities in the samples and confirmed the presence of the dopants in the samples [11,13-17]. Figures 5A-K show the energy dispersive analysis x-ray (EDAX) mapping images of the nanoparticles. From the EDAX mapping images it is clear that the nanoparticles contained all the elements and were homogeneously distributed. The morphology of the prepared nanoparticles was studied using FESEM. The FESEM micrographs are shown in Figures 6A-D which reveal further

information about the morphology of the samples. From the FESEM micrographs, it is clear that the prepared nanoparticles were spherical in shape and of different sizes.

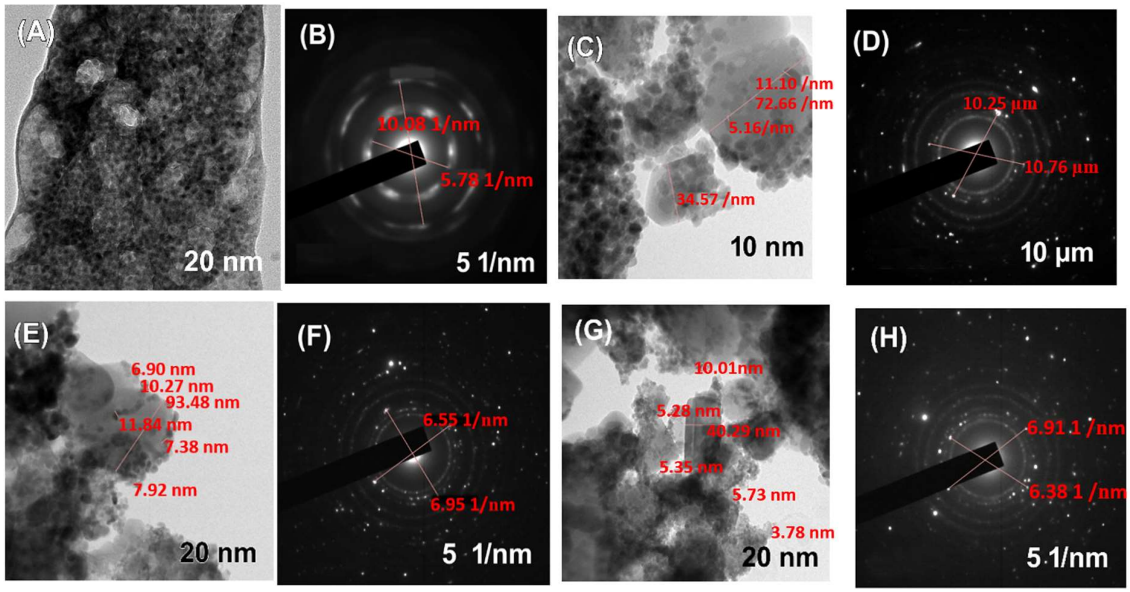

Figure 3 TEM image and SAED pattern of (A, B) ZnO, (C, D) ZnO: Th, (E, F) ZnO Th: Mg, and (G, H) ZnO: Th Ca.

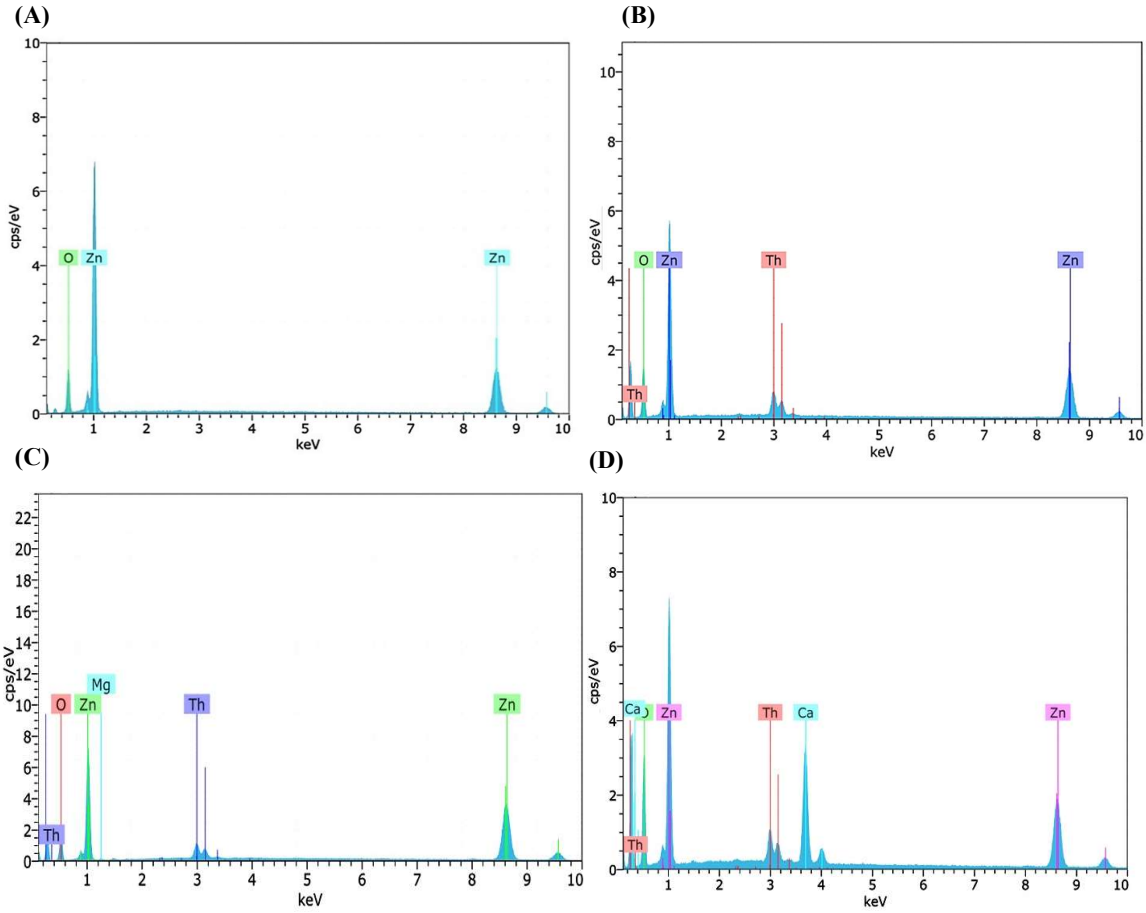

Figure 4 Displays the EDX spectra of the prepared nanoparticles: (A) ZnO: Th, (B) ZnO: Th: Mg, (C) ZnO: Th: Ca and (D) ZnO.

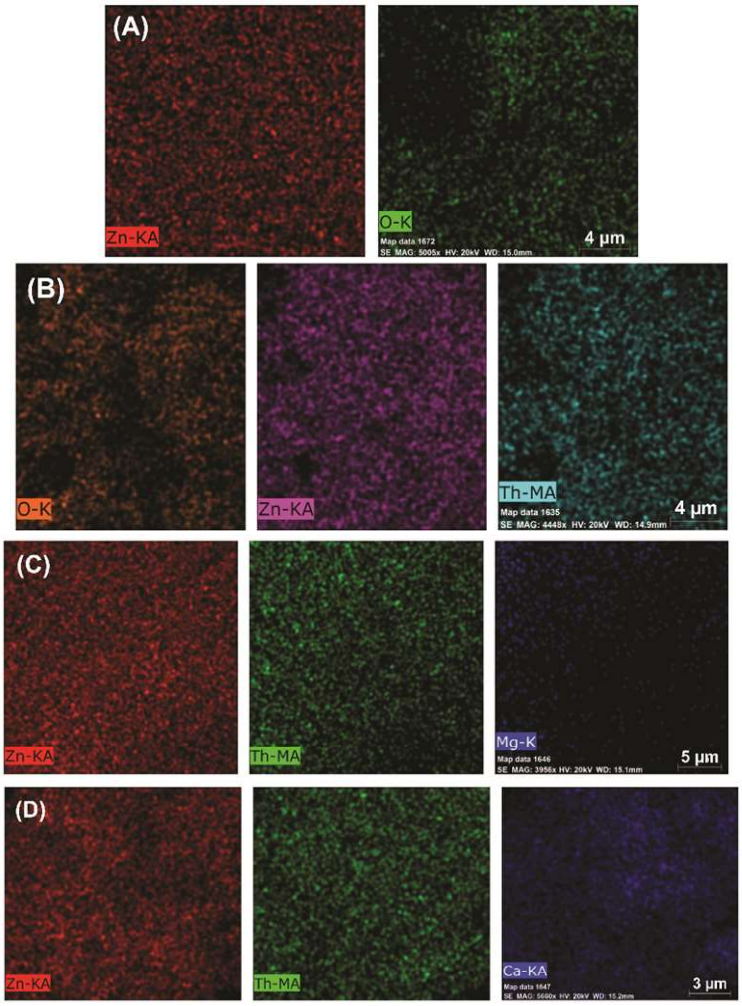

Figure 5 EDX elemental mapping of (A) 100 % ZnO containing 80.68 % Zinc and 19.32 % Oxygen, (B) 90:10 % ZnO: ThO_2 sample containing 70.27 % Zinc, Thorium 10.82 % and Oxygen 18.91 % by weight, (C) 90:6:4% ZnO: ThO_2: MgO sample with Zinc 77.88%, Thorium 7.07 %, Magnesium 3.76 % and Oxygen 11.29%, and (D) 90:6:4% ZnO: ThO_2: CaO sample with Zinc 77.38%, Thorium 6.29 %, Magnesium 3.55 % and Oxygen 12.78%.

The elemental mapping suggests that the prepared nanoparticles composed of Zinc and O_2 in ZnO nanoparticle, Zinc, Th and O_2 in Th doped ZnO nanoparticle, Zinc, Th, Mg and O_2 in Th / Mg doped ZnO nanoparticle and Zinc, Thorium, Ca and O_2 in Th Ca doped ZnO nanoparticle respectively. This shows that our synthesized nanoparticles are pure and contain no impurity elements other than the synthesised ones. This is further complemented by the EDX images. Furthermore, from the mapping images shown, it is clear that the elements are evenly distributed throughout the samples and localization of any element is not observed.

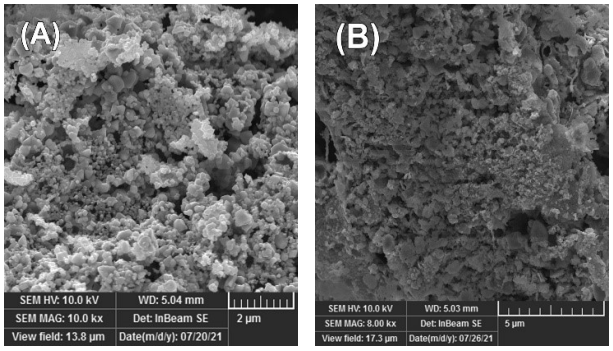

Figure 6 FESEM images of (A) ZnO, and (B) ZnO: Th.

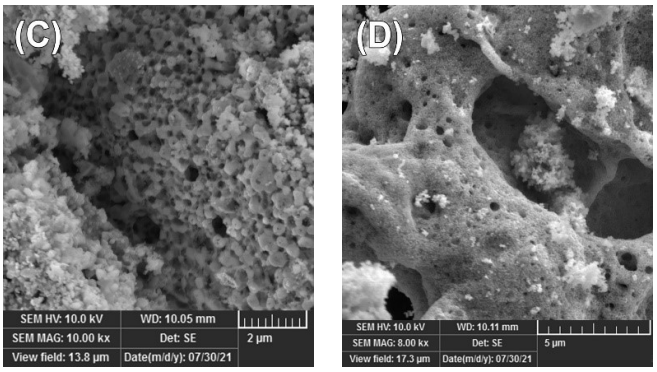

Figure 6 (Continued) FESEM images of (C) ZnO: Th: Mg, and (D) ZnO: Th: Ca.

3.4 Optical properties UV-vis NIR spectroscopy

The optical absorption and transmission were conducted in the range 200 to 1000 nm by UV-visible NIR spectroscopy. The UV-visible spectra revealed a broad peak for pure ZnO sample around 372 nm, and this was in accordance with the published data. The absorption peaks of the doped samples shifted towards the higher wavelengths, that is red shift, supporting the presence of doping concentrations [16-17,19]. The absorption and transmittance spectra are shown in Figure 7A. The band gap was calculated using the Equation.

$$Eg = h\,c\,/\lambda\,e\ (eV) \tag{3}$$

where Eg is the band gap, λ is the UV-vis absorption peak wavelength in nm, e is the electron charge, h is the Planck's constant, c is the velocity of light [10]. The band gap was also calculated using Tauc's plot, as shown in Figure 7B, which represents the variation of $(ahv)^2$ *vs*. photon energy (hv), where the X-intercept of the tangent denotes the direct Eg in eV. Here hv = hc/λ, a is the adsorption coefficient. Table 3 displays the calculated values of the band gap thus calculated. The band gap of pure ZnO was found to be 3.33 eV. With the addition of the dopants the band gap got reduced. Thus, we can conclude that the addition of metal oxides to ZnO increases the photocatalytic activity of pure ZnO samples.

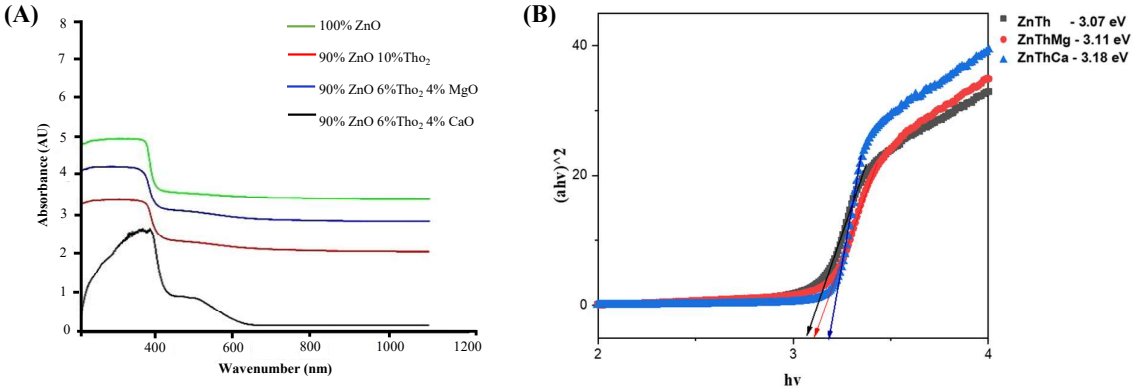

Figure 7 (A) UV absorption spectra and transmittance spectra (inset) of the samples, and (B) Tauc's plot.

Table 3 Calculated band gap.

Samples	Observed absorption wavelength (nm)	Calculated Eg (eV)
100% ZnO	372	3.33
Th doped ZnO	405	3.07
Th / Mg co-doped ZnO	399	3.11
Th / Ca co-doped ZnO	391	3.18

3.5 Surface morphological studies- atomic force microscopy

AFM studies were conducted for pure ZnO and ZnO: Th samples, to further investigate the surface morphology, distribution of the crystallites and growth patterns [20-22]. Figure 8A-D shows the 3D and 2D profile of the synthesized samples. The size distributions of these samples are shown in Figures 9A-B. As seen

in the graph, the particle size for pure ZnO varied in the range 40 to 100 nm, and when doped with thorium it got reduced to 5 to 30 nm range.

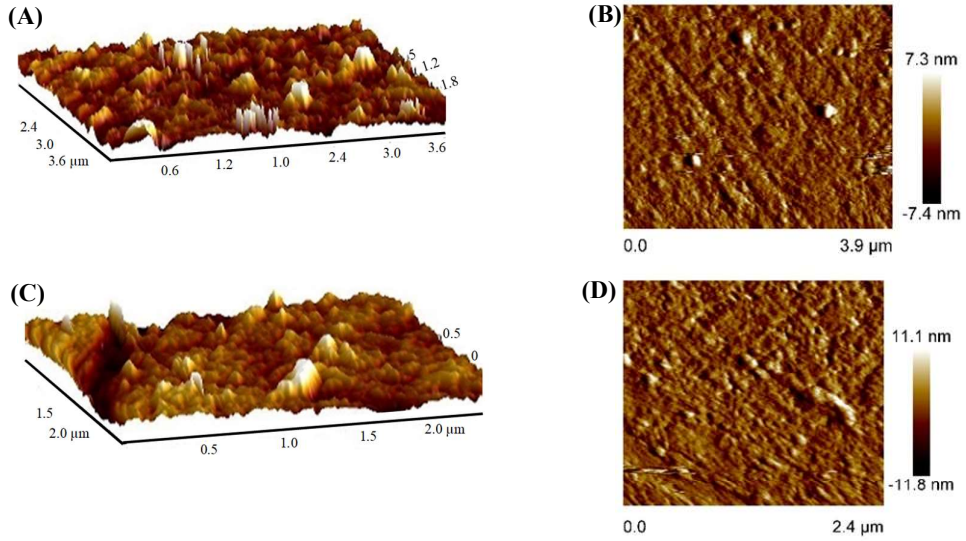

Figure 8 (A) 3D profile of pure ZnO, (B) 2D profile of pure ZnO, (C) 3D profile of ZnO: Th, and (D) 2D profile of ZnO: Th.

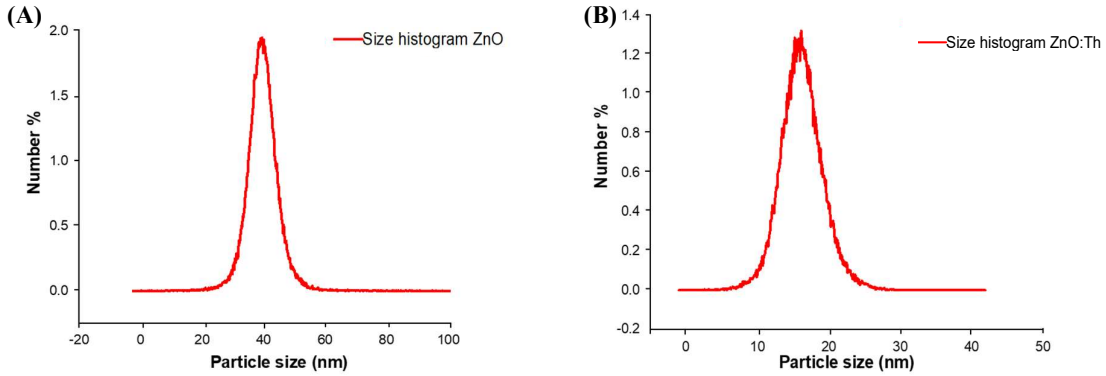

Figure 9 (A) Size distribution of ZnO nano particles, and (B) size distribution of ZnO: Th nano particles.

3.6 Chemical composition studies- x- ray photoelectron spectroscopy

XPS studies were conducted for ZnO: Th: Ca sample, to study the chemical composition and valency of the Th-Ca co-doped sample. The XPS spectra of Ca, Zn, Th and O in the sample are indicated in Figure 10A-E. The Zn2p spectra exhibit peaks of $Zn2p_{3/2}$ and $Zn2p_{1/2}$ at 1021.9 eV and 1045 eV respectively, thus showing a difference of 23.1 eV between the states as per literatures [2,20]. This indicates that the Zn element exists in the form of Zn^{2+} state in the sample. The O_2 scan shows a peak of 530.4 eV, which can be attributed to O^{2-} ions in the samples. The broad peak indicates all the instances of O_2 bonding in the sample. The Th 4f spectrum displays peak binding energy at 333.7 eV and 342 eV, denoting Th $4f_{7/2}$ and Th $4f_{5/2}$ respectively [18]. Ca 2p spectrum displays the prime binding energy peak at 342 eV [22,23] and C 1s at 284.8 eV. Table 4 shows the peak binding energy of the elements in ZnO: Th: Ca sample.

Table 4 Binding energy from XPS analysis.

ZnO: Th: Ca sample	Peak binding energy (eV)
$Zn2p_{3/2}$	1021.9
$Zn2p_{1/2}$	1045.0
$Th4f_{7/2}$	333.7
$Th4f_{5/2}$	342.0
Ca2p	342.0
O1s	530.4

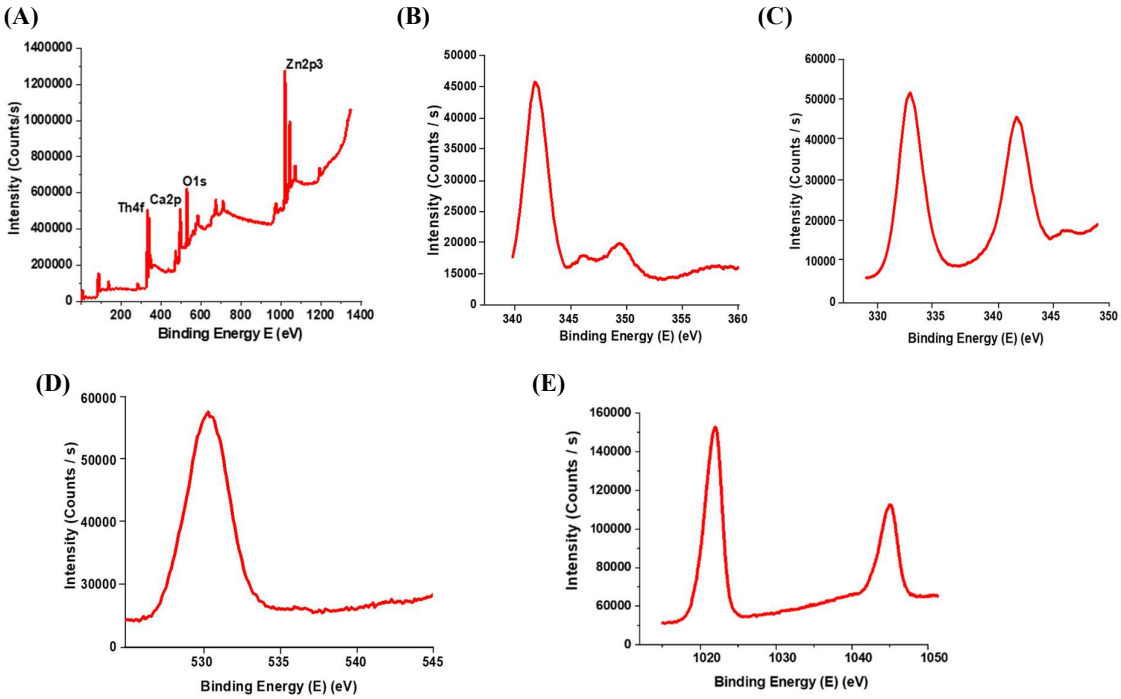

Figure 10 (A) Survey scan of ZnO: Th: Ca sample, (B) Binding energy Ca 2p ZnO: Th: Ca sample, (C) Binding energy Th 4f ZnO: Th: Ca sample, (D) Binding energy O 1s ZnO: Th: Ca sample, and (E) Binding energy Zn 2p ZnO: Th: Ca sample.

4. Conclusion

Metal oxide nanoparticles have many unique properties and can be customized to our advantage through proper engineering of the shape and size, thereby optimizing their properties. To summarize, in the present work, pure and transition metal Th and alkaline earth metal (Mg and Ca) doped ZnO were prepared by solution combustion synthesis method and studied for their morphology as well as structural and optical properties. It was found that the average grain size got reduced to 20 nm when doped with Th, while co-doped with Mg and Ca, the grain size of pure ZnO decreased further even while it maintained the crystallinity at 24.63 nm and 28.6 nm respectively. The XRD and TEM data confirm the crystallinity of the samples. It also explained that the hexagonal structure of the major ZnO is retained even when it is doped. The FESEM/EDX studied the elemental composition and purity of the samples and confirmed the presence of Zn, Th, Mg, Ca, O elements respectively. The UV spectra indicated the absorption spectra at around 372 nm which is the fingerprint absorption peak of ZnO. Thus, by doping rare earth metal Th, the optical properties of ZnO nanoparticles are improved and co-doping with alkaline earth metals both the electrical and optical properties are enhanced. The XPS spectra pointed to the respective binding energies of the elements, and the AFM revealed their surface morphology. Thus, the synthesis of a multifunctional nano particle using environment-friendly solution combustion synthesis method is achieved. These results point out that the synthesis method is a very simple, fast, low-temperature process which can be adopted for mass production.

5. Acknowledgements

The authors are thankful to the authorities concerned for providing the testing facilities at Cochin University (STIC), Cochin, (CSIF) University of Calicut, NIIT Calicut and CLIF, University of Kerala.

6. References

[1] Bindu P, Sabu T. Estimation of lattice strain in ZnO nanoparticles: x-ray peak profile analysis. J Theor Appl Phys. 2014;8:123-134.

[2] Shivananjaiah HN, Kumari KS, Geetha MS. Green mediated synthesis of lanthanum doped zinc oxide: study of its stuctural, optical and latent fingerprint application. J Rare Earths. 2020;38:1281-1287.

[3] Varma A, Mukasyan AS, Rogachev AS, Manukyan KV. Solution combustion synthesis of nanoscale materials. Chem Rev. 20016;116:14493-14586.

[4] Rashid M, Ikram M, Haider A, Naz S, Haider J, Hamid AU, et al. Photocatalytic, dye degradation, and bactericidal behavior of Cu-doped ZnO nanorods and their molecular docking analysis. Dalton Trans. 2020;49(24):8314-8330.

[5] Ali M, Sharif S, Anjum S, Imran M, Ikram M, Naz M, et al. Preparation of Co and Ni doped ZnO nanoparticles served as encouraging nano-catalytic application. Mater Res Express. 2019;6(12):1250d5.

[6] Afzal H, Ikram M, Ali S, Shahzadi A, Aqeel M, Haider A, et al. Enhanced drug efficiency of doped ZnO-GO (graphene oxide) nanocomposites, a new gateway in drug delivery systems (DDSs). Mater Res Express. 2020;7(1):015405.

[7] Shaheen S, Iqbal A, Ikram M, Imran M, Naz S, Hamid AU, et al. Graphene oxide-ZnO nanorods for efficient dye degradation, antibacterial and in-silico analysis. Appl Nanosci. 2022;12:165-177.

[8] Ikram M, Mahmood A, Haider A, Naz S, Hamid AU, Nabgan W, et al. Dye degradation, antibacterial and in-silico analysis of Mg/cellulose-doped ZnO nanoparticles. Int J Biol Macromol. 2021;185:153-164.

[9] Ikram M, Aslam S, Haider A, Naz S, Hamid AU, Shahzadi A, et al. Doping of Mg on ZnO nanorods demonstrated improved photocatalytic degradation and antimicrobial potential with molecular docking analysis. Nanoscale Res Lett. 2021;16(1):1-16.

[10] Bhaskar P, Veena MG, Madhukar BS. Synthesis and experimental investigation of zinc oxide and praseodymium oxide fused metal oxide nanostructures. In: Bartolomeo AD, Jeske MC, editors. IEEE 21st International Conference on Nanotechnology NANO; 2021 Jul 28-30; Montreal, Canada. New Jersey; IEE Xplore; 2021, p. 104-107.

[11] Panneerselvam G, Antony MP, Vasudevan T. A study on ThO2-LaO1.5 solid solution: lattice thermal expansion measurements and XPS studies. J Alloys Compd. 2006;415(1):26-30.

[12] Parangusan H, Ponnamma D, Maadeed MA. Effect of cerium doping on the optical and photocatalytic properties of ZnO nanoflowers. Bull Mater Sci. 2009;42(179):1-11.

[13] Hembram K, Rao TN, Ramakrishana M, Srinivasa RS, Kulkarni AR. Influence of CaO doping on phase, microstructure, electrical and dielectric properties of ZnO varistors. J Alloys Compd. 2020;817:152700.

[14] Martínez JA, Rodríguez E, Villarreal SG, Franco LF, Hernandez MB. Effect of Ca, Sr and Ba on the structure, morphology and electrical properties of Co, Sb -doped SnO_2 varistors. Mater Chem Phys. 2015;153:180-186.

[15] Asikuzun E, Donmez A, Arda L, Cakiroglu O, Ozturk O, Akcan D, et al. Structural and mechanical properties of (Co/Mg) co-doped nano ZnO. Ceram Int. 2015;41(5):6326-6334.

[16] Brimhall NF, Grigg AB, Turley RS, Allred D. Thorium dioxide thin films in the extreme ultraviolet. Proc Soc Photo-opt Instrum Eng. 2006;6317:10-11.

[17] Ebrahimi R, Hossienzadeh K, Ghanbari AM, Puttaiah SH. Effects of doping ZnO nanoparticles with transition metals on photocatalytic degradation of direct blue 15 dye under uv and visibnle irradiation. J Environ Health Sci Eng. 2019;17:479-492.

[18] Abdullah KA, Awad S, Zaraket J, Salame C. Synthesis of ZnO nanopowders by using sol-gel and studying their structural and electrical properties at different temperature. Energy Procedia. 2017;119:565-570.

[19] Kumar H, Rani R. Structural and optical characterization of zno nanoparticles synthesized by microemulsion route. Int Lett Chem Phys Astron. 2013;19:26-36

[20] Lu W, Zhu D. Synthesis and characterization of La-Ce codoped polycrystal ZnO prepared by hydrothermal method for 1,2 propanediol. Appl Phys. 2019;68:1-9.

[21] Vignesh K, Rajarajan M, Suganthi A. Visible light assisted photocatalytic performance of Ni and Th co-doped ZnO nanoparticles for the degradation of methylene blue dye. J Ind Eng Chem. 2014;20(5):3826-3833.

[22] Sree GV, Nagaraaj P, Kalanidhi K, Aswathy CA, Rajasekaran P. Calcium oxide a sustainable photocatalyst derived from eggshell for efficient photodegradation of organic pollutants. J Clean Prod. 2020;270:1222294.

[23] Fujimori Y, Zhao X, Shao X, Levchenko SV, Nilius N, Sterrer M, et al. Interaction of water with the CaO(001) surface. J Phys Chem. 2016;120(10):5565-5576.